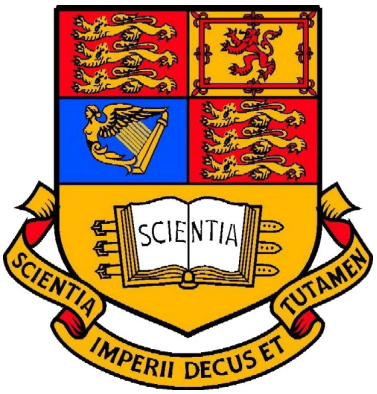

CDT on Theory and Simulation of Materials

Imperial College London

Group Programming Project

Tight-Binding Molecular Dynamics Simulation of Carbon Compounds

Authors:
Lars Blumenthal, Luca Cimbaro, Hikmatyar Hasan, Behnam Najafi, Eduardo Ramos Fernandez, Gleb Siroki

Supervisors:
Prof. Peter D. Haynes, Dr. James Spencer

2014/15

Abstract

A molecular dynamics program coupled to a semi-empirical tight-binding code was written to investigate the time evolution of carbon structures. Properties, such as normal modes, heat capacities, equilibrium bond lengths and elastic constants were calculated for a range of carbon structures. The structures investigated include small carbon clusters, Buckminsterfullerene, diamond and nanotubes. The properties of the structures were verified with both experimental data and other more recent methods such as Density Functional theory. Some properties, such as the normal modes of Buckminsterfullerene and certain linear chains were in good agreement with literature values. On the other hand, the Youngs modulus of the carbon nanotube was not in agreement with the experimental data.

Acknowledgments

We are thankful to Peter Haynes & James Spencer for their expertise. We would also like to thank the other members of our Cohort for the insightful discussions regarding the Group programming project.

Contents

List of Figures

Chapter 1

Introduction

The aim of the project was to create a molecular dynamics program that evolves a system of carbon atoms interacting via a semi-empirical tight-binding potential. The program written, is able to describe time evolution and relaxation of finite or periodic structures to their equilibrium configurations. This can be used to calculate quantities such as equilibrium bond lengths, elastic constants normal modes and heat capacities, among others. Calculations can be performed for a range of temperatures, using the OVRVO thermostat. The details of its implementation are given in [8]. The quantities obtained from calculations can be verified against experimental data or more sophisticated methods such as Density Functional Theory (DFT) and Many Body Perturbation Theory (MBPT).

We investigated finite structures such as small carbon cluster and Buckminsterfullerene ($C60$) as well as periodic structure including a linear chain of C atoms, diamond, graphene and single-walled carbon nanotube. Structures consisting of benzene rings (nanotubes and graphene) can be generated within the program.

The next section reviews the theoretical background necessary to calculate the quantities above. This is followed by a section describing the implementation of the theoretical results in the current program. Results are then discussed and finally conclusions are made pertaining to the effectiveness of the program.

Chapter 2

Theory

2.1 Integrators and Thermostats

2.1.1 Molecular Dynamics

The molecular dynamics (MD) simulation serves dual purpose of relaxing the system of carbon atoms towards the equilibrium configuration as well as allows studying dynamical behaviour. For the purpose of relaxation the atoms in the initial structure are assigned zero velocities and are allowed to move down the energy gradient and damping force is introduced in the equation of motion which for atom i reads as

$$m\ddot{\mathbf{r}}_i = \mathbf{f}_i - \gamma\dot{\mathbf{r}}_i, \tag{2.1}$$

where $\mathbf{r}_i$ is the position of atom i, m is the mass of the carbon atom (C-12 isotope mass is used throughout in the code), $\mathbf{f}_i$ is gradient force acting on atom i and $\gamma\dot{\mathbf{r}}$ is the damping force where γ is a positive damping constant. The steepest descent method used for relaxation may lead to a local minimum in total energy however this can be avoided by using different initial configurations. The method also leads to slow convergence in case of difficult energy landscapes but this is compensated by simplicity and reliability of the method.

For periodic structures such as diamond, periodic boundary conditions were implemented. However, during the relaxation of periodic structures lattice parameter cannot change. Therefore, the equilibrium lattice parameters and bond lengths in such cases were found by locating the minimum of the cohesive energy in static calculations.

Lastly, it can be noted that the system of carbon atoms is conservative when the damping constant is zero, in which case the system's total energy is conserved because of time invariance. However, energy fluctuations are expected since the integration of the deterministic equations of motion is discrete. These fluctuations thought can be reduced by using a smaller time step.

2.1.2 Thermostat

The thermostat which was used for the MD simulations in the canonical (NVT) ensemble is referred to as OVRVO [8]. It is a stochastic generalisation of the Velocity Verlet algorithm. The name is not a deliberate tongue twister but indicates the following: the O represents a stochastic thermalisation step employing an Ornstein-Uehlenbeck operator while the V and the R stand for a discrete (deterministic) evolution of the velocities and coordinates of the atoms in the system, respectively.

In the case of a time-independent Hamiltonian, the OVRVO consists of five steps. For an exact description of these steps, we refer to the original paper, Ref. [8], and the `ParticleSystem.cpp` file where the integration is realised within our code. Credits are also given to Tangney [10] whose MATLAB implementation of the code strongly influenced our implementation of the thermostat.

One of the advantages for choosing OVRVO is its ability to be straightforwardly converted into many other integrators by adjusting the relevant parameters [8]. For example, one can easily obtain the velocity Verlet algorithm or overdamped Langevin dynamics by merely changing the friction coefficient γ. It also outperformed all the five other velocity Verlet with velocity randomisation thermostats [8]. Although not used for the results discussed in this report, one could easily use the time step rescaling option OVRVO which allows to obtain the correct root mean square displacement of particles in a force free system, as shown by Sivak et al [8], or to maximise the time step used within the MD simulation. Additionally, Sivak et al also demonstrated that the energy error associated with the use of OVRVO is of second order in Δt.

2.2 Tight-Binding

The forces experienced by atoms as calculated in molecular dynamics simulation have two contributions. Forces due to interaction of valence electrons with nuclei are described with tight-binding model. Another force that arises when valence electrons of one atom approach the core electrons of another atom and feel Pauli repulsion will be covered in the next section. Born-Oppenheimer approximation is applied throughout and we assume that the system remains in ground electronic state. The aim of the tight-binding model is to solve the Schrödinger equation for an interacting system of N atoms:

$$\hat{H}\,|\psi\rangle = \epsilon\,|\psi\rangle\ , \tag{2.2}$$

where $\hat{H}$ is the Hamiltonian of the system, ϵ is the eigenvalue. $|\psi\rangle$ is the wave-function of the system which is taken to be a linear combination of atomic orbitals (LCAO)

$$|\psi\rangle = \sum_{i=0}^{N-1} \sum_{\alpha} c_{i\alpha}\,|\phi_{i\alpha}\rangle\,, \tag{2.3}$$

where $c_{i\alpha}$ are expansion coefficients, i defining the atomic site and α - the type of orbital. Each carbon atom has four valence electrons per atom and four distinct orbitals, namely s, p_x, p_y and p_z. The expansion for the wave function above can be substituted into the Schrodinger equation (2.2) to arrive at the following generalised eigenvalue problem.

$$H_{i\alpha j\beta}\,c^s_{j\beta} = \epsilon^s S_{i\alpha j\beta}\,c^s_{j\beta}\,, \tag{2.4}$$

where $H_{i\alpha j\beta} = \left\langle \phi_{i\alpha} \middle| \hat{H} \middle| \phi_{j\beta} \right\rangle$ denote the matrix elements of the Hamiltonian, $S_{i\alpha j\beta} = \langle \phi_{i\alpha} |\ \phi_{j\beta}\rangle$ is the overlap matrix and ϵ^s is the eigenvalue belonging to the vector of coefficients $\mathbf{c}^s$. A further approximation is now made by equating overlap matrix to the identity. This leads to a simpler eigenvalue problem:

$$H_{i\alpha j\beta}\,c^s_{j\beta} = \epsilon^s\,c^s_{i\alpha}\,, \tag{2.5}$$

This equation can be solved once the matrix elements $H_{i\alpha j\beta}$ are known. These elements come in two flavours - so called on-site elements that describe the interaction of electrons with the nucleus they belong to and hopping elements that describe probability of electron being transferred from one atom to another. The on site elements correspond to the case $i = j$ in which case the matrix elements are given by

$$H_{i\alpha i\beta} = E_\alpha \delta_{\alpha\beta}\,, (no\ sum) \tag{2.6}$$

where values of $E_s =$ and $E_{p_x} = E_{p_y} = E_{p_z}$ parameters were taken from [11]. These values reflect the fact that s-orbitals are lower in energy while proportionality follows from the fact that the orbitals s, p_x, p_y and p_z are orthogonal [9].

In the case of hopping elements ($i \neq j$) the values of matrix elements depend on relative positions of a pair of atoms $\mathbf{r}_i$ and $\mathbf{r}_j$ respectively. We now define $\mathbf{d}_{ij} = (\mathbf{r}_i - \mathbf{r}_j)/\left|\mathbf{r}_i - \mathbf{r}_j\right|$. Also let $\mathbf{a}_q$ be the cartesian unit vector $\hat{\mathbf{x}}$, $\hat{\mathbf{y}}$ and $\hat{\mathbf{z}}$ for $q = x, y$ and z respectively, and let $\mathbf{n}_{ij}$ be a normal vector to $\mathbf{d}_{ij}$.

For two types of orbitals that have distinct symmetry (s and p) and two possible orientations of p orbital (along the bond direction and perpendicular to it) there are correspondingly four types of hoppings to be considered. Each of these hoppings are scaled to by the same function proposed by [11] that accounts for the fact that probability of electron transfer between two atoms increases as they get closer together.

The first of the four hopping integrals represents the interaction between two atomic orbitals s and is given by the following expression

$$H_{isjs} = \left\langle \phi_{is} \right| \hat{H} \left| \phi_{js} \right\rangle = h_{ss\sigma}\, s(r_{ij})\,, \tag{2.7}$$

where $h_{ss\sigma}$ is another parameter taken from [11] (as well as ones below) and $s(r_{ij})$ is the scaling function that depends only on distance between atoms i and j.

The second hoping integral describes interaction of the s orbital of the atom i interacting with the p orbital on atom j along the q direction in which case $\left|\phi_{ip_q}\right\rangle$ can be decomposed into contributions parallel and perpendicular to the bond.

$$\left|\phi_{ip_q}\right\rangle = \mathbf{a}_q \cdot \mathbf{d}_{ji} \left|\phi_{ip_{\mathbf{d}}}\right\rangle + \mathbf{a}_q \cdot \mathbf{n}_{ji} \left|\phi_{ip_{\mathbf{n}}}\right\rangle\,, \tag{2.8}$$

where $\left|\phi_{ip_{\mathbf{d}}}\right\rangle$ and $\left|\phi_{ip_{\mathbf{n}}}\right\rangle$ represent the p orbital of the atom i interacting with the atom j along the direction $\mathbf{d}_{ji}$ and $\mathbf{n}_{ji}$ respectively. Then it follows that the matrix element $H_{isjp_q} = \left\langle \phi_{is} \right| \hat{H} \left| \phi_{jp_q} \right\rangle$ is given by

$$H_{isjp_q} = \mathbf{a}_q \cdot \mathbf{d}_{ij} \left\langle \phi_{is} \right| \hat{H} \left| \phi_{jp_{\mathbf{d}}} \right\rangle\,, \tag{2.9}$$

where q defines a Cartesian direction [9]. It can be noted that there is no contributions from the normal component of the p orbital, $\left|\phi_{ip_{\mathbf{n}}}\right\rangle$, because it is zero by symmetry. The expectation value $\left\langle \phi_{is} \right| \hat{H} \left| \phi_{jp_{\mathbf{d}}} \right\rangle$ is the second hoping integral and it represents the interaction between the atomic orbitals s and p_q . Its expression is given by

$$\left\langle \phi_{is} \right| \hat{H} \left| \phi_{jp_{\mathbf{d}}} \right\rangle = h_{sp\sigma}\, s(r_{ij})\,, \tag{2.10}$$

Finally we discuss the remaining two integrals describing hopping between p orbitals. From equation (2.8), it follows that the matrix element that:

$$H_{ip_l jp_q} = (\mathbf{a}_l \cdot \mathbf{d}_{ij})(\mathbf{a}_q \cdot \mathbf{d}_{ij}) \left\langle \phi_{ip_{\mathbf{d}}} \right| \hat{H} \left| \phi_{jp_{\mathbf{d}}} \right\rangle + \Big(\mathbf{a}_l - (\mathbf{a}_l \cdot \mathbf{d}_{ij})\mathbf{d}_{ij}\Big) \cdot \Big(\mathbf{a}_q - (\mathbf{a}_q \cdot \mathbf{d}_{ij})\mathbf{d}_{ij}\Big) \left\langle \phi_{ip_{\mathbf{n}}} \right| \hat{H} \left| \phi_{jp_{\mathbf{n}}} \right\rangle \tag{2.11}$$

where q and l represent the Cartesian axes x, y and z. In order to obtain the equation (2.11), it has been used the orthogonality of the p orbitals [9]. Where

$$\left\langle \phi_{ip_{\mathbf{d}}} \right| \hat{H} \left| \phi_{jp_{\mathbf{d}}} \right\rangle = h_{pp\sigma}\, s(r_{ij})\,, \tag{2.12}$$

And

$$\left\langle \phi_{ip_{\mathbf{n}}} \right| \hat{H} \left| \phi_{jp_{\mathbf{n}}} \right\rangle = h_{pp\pi}\, s(r_{ij})\,, \tag{2.13}$$

To sum up, the total Hamiltonian of the system can be split diagonal 4x4 sub-blocks that describe on-site energies

$$\begin{pmatrix} E_s & 0 & 0 & 0 \\ 0 & E_{p_x} & 0 & 0 \\ 0 & 0 & E_{p_y} & 0 \\ 0 & 0 & 0 & E_{p_z} \end{pmatrix}, \tag{2.14}$$

and off-diagonal 4x4 sub-blocks that describe interactions between pairs of atoms. For examples, given interaction of atom i with atom j such sub-block would take the form:

$$\begin{pmatrix} h_{ss\sigma} & d_{x_{ij}} h_{sp\sigma} & d_{y_{ij}} h_{sp\sigma} & d_{z_{ij}} h_{sp\sigma} \\ -d_{x_{ij}} h_{sp\sigma} & d_{x_{ij}}^2 h_{pp\sigma} + \big(1 - d_{x_{ij}}^2\big) h_{pp\pi} & d_{x_{ij}} d_{y_{ij}} (h_{pp\sigma} - h_{pp\pi}) & d_{x_{ij}} d_{z_{ij}} (h_{pps} - h_{pp\pi}) \\ -d_{y_{ij}} h_{sp\sigma} & d_{y_{ij}} d_{x_{ij}} (h_{pp\sigma} - h_{pp\pi}) & d_{y_{ij}}^2 h_{pp\sigma} + \big(1 - d_{y_{ij}}^2\big) h_{pp\pi} & d_{y_{ij}} d_{z_{ij}} (h_{pp\sigma} - h_{pp\pi}) \\ -d_{z_{ij}} h_{sp\sigma} & d_{z_{ij}} d_{x_{ij}} (h_{pps} - h_{pp\pi}) & d_{z_{ij}} d_{y_{ij}} (h_{pp\sigma} - h_{pp\pi}) & d_{z_{ij}}^2 h_{pp\sigma} + \big(1 - d_{z_{ij}}^2\big) h_{pp\pi} \end{pmatrix} s(r_{ij}), \tag{2.15}$$

The forces arising from the tight-binding Hamiltonian described above are calculated using the Hellman-Feynman theorem which states that the force on atom k is given by:

$$\begin{aligned} \mathbf{f}_k &= \sum_s -2 n_s \nabla_k \epsilon^s \\ &= \sum_s -2 n_s (c_{i\alpha}^s)^* c_{j\beta}^s \nabla_k H_{i\alpha j\beta}, \end{aligned} \tag{2.16}$$

where n_s is the occupancy of the state s with the eigenvalue ϵ^s and the factor 2 is due to the spin degeneracy of the orbitals [2]. As mentioned above the system is assumed to be in its ground state so that the states s are populated with all electrons of the system starting from the lowest eigenvalue. In addition, because Hamiltonian matrix is real and symmetric it follows that eigenvectors can be chosen to be real in which case one can drop the complex conjugate label in expression above.

2.3 Repulsive Forces

The total energy of the system can be written as:

$$E = E_{bond} + E_{rep}\,, \tag{2.17}$$

where E_{bond} gives rise to forces explained in the previous section and E_{rep} is added to compensate for the difference between E_{bond} and *ab initio* results. The physical motivation behind E_{rep} stems from the fact that the discussion in the previous section only includes the valence electrons. However, when the atoms are brought close together, we expect the cores to repel each other in a pairwise fashion. Therefore, one can think of E_{rep} as enforcing both the core-core repulsion and the non-local binding in the lattice. We follow the definition of the repulsive energy term given by Xu et al [11].

$$E_{rep} = \sum_{i=0}^{N-1} E_{rep}^{(i)}[\phi(r_{ij})] = \sum_{i=0}^{N-1} f\Big(\sum_{j=nn(i)} \phi(r_{ij})\Big) = \sum_{i=0}^{N-1} f(A_i), \tag{2.18}$$

where $nn(i)$ denotes the number of neighbours to atom i, and the functional $E_{rep}^{(i)}[\phi]$ is represented as a 4th-order polynomial function, $f(A_k)$ where:

$$A_k = \sum_{j=nn(k)} \phi(r_{kj}). \tag{2.19}$$

The coefficients of the fourth order polynomial are chosen by fitting to *ab initio* LDA results for a range of Carbon systems [3]. The inter-atomic repulsive potential term $\phi(r_{ij})$ can be calculated between each pair using the expression given by Xu et al [11], with the exponential tail smoothly brought to zero using a 3rd-order polynomial $t_\phi(r_{ij} - r_1)$, where r_1 is the match radius. Once E_{rep} is known, we calculate the forces on atom k by:

$$\mathbf{F}_{rep}^{(k)} = -\frac{\partial E_{rep}}{\partial x_k}\mathbf{i} - \frac{\partial E_{rep}}{\partial y_k}\mathbf{j} - \frac{\partial E_{rep}}{\partial z_k}\mathbf{k}. \tag{2.20}$$

These derivatives can be evaluated using the chain rule:

$$\frac{\partial E_{rep}}{\partial x_k} = \sum_i \frac{df}{dA_i}\frac{\partial A_i}{\partial x_k} = \sum_{i,j=nn(i)} \frac{df}{dA_i}\frac{d\phi(r_{ij})}{dr_{ij}}\frac{\partial r_{ij}}{\partial x_k}, \tag{2.21}$$

where $\frac{\partial r_{kj}}{\partial x_k}$ is just the directional cosine of the separation between atoms i and j in the x-direction. Similar expressions can be obtained for the other Cartesian axes.

2.4 Relaxation and Normal modes

The initial input structure need to be relaxed to obtain equilibrium configurations for a given number of carbon atoms. This is achieved using steepest descent method, i.e. allowing atoms to move down the energy gradient with an applied damping. Once the equilibrium structure is obtained in this manned for a given number of carbon atoms its normal modes can be computed. Let $\mathbf{x}_i^{\text{eq}}$, $i = 0, \ldots, N-1$ denote equilibrium positions for a system of N carbon atoms. If the

position of the atom i is denoted by $\mathbf{x}_i = (x_i^1, x_i^2, x_i^3)$, $i = 0, \ldots, N-1$. Now the Lagrangian of the system can be expressed as

$$\mathcal{L} = \frac{m}{2}\sum_{i=0}^{N-1}\dot{\mathbf{x}}_i^2 - \frac{1}{2}\sum_{i,j=0}^{N-1}(\mathbf{x}_i - \mathbf{x}_i^{\mathrm{eq}})D_{ij}(\mathbf{x}_j - \mathbf{x}_j^{\mathrm{eq}}), \tag{2.22}$$

where D_{ij} is the dynamical matrix whose elements are given by

$$\big(D_{ij}\big)_{\alpha\beta} = \left.\frac{\partial^2 E}{\partial x_i^\alpha \partial x_j^\beta}\right|_{(\mathbf{x}_0^{\mathrm{eq}},\ldots,\mathbf{x}_{N-1}^{\mathrm{eq}})}, \tag{2.23}$$

where $\alpha, \beta = x, y, z$ and E represents the total energy of the system. Extremising the Lagrangian leads to the Euler-Lagrange equations of motion:

$$m\ddot{\mathbf{X}}_i + \sum_{j=0}^{N-1} D_{ij}\mathbf{X}_j = 0, \qquad \forall i = 0, \ldots, N-1 \tag{2.24}$$

where $\mathbf{X}_i = \mathbf{x}_i - \mathbf{x}_i^{\mathrm{eq}}$. The normal modes can be obtained by substituting $\mathbf{X}_i = \mathbf{X}_i^0 e^{i\omega t}$ into (2.24) leading to the following eigenvalue problem

$$\frac{D_{ij}}{m}\mathbf{X}_j^0 = \omega^2 \mathbf{X}_i^0 \tag{2.25}$$

where ω is the normal frequency and corresponding to the eigenvector $\mathbf{X}_0 = (\mathbf{X}_0^0, \ldots, \mathbf{X}_0^{N-1})$.

The D_{ij} matrix can be evaluated by the method of small displacements which applies numerical central finite difference formula to the forces

$$\big(D_{ij}\big)_{\alpha\beta} = \frac{f_j^\beta(\mathbf{x}_i^{\alpha\mathrm{eq}} - h) - f_j^\beta(\mathbf{x}_i^{\alpha\mathrm{eq}} + h)}{2h}, \tag{2.26}$$

where $\mathbf{f}_j = (f_j^x, f_j^y, f_j^z)$ is the force on the atom j and coordinates not mentioned explicitly above take their equilibrium values. h is a small number that should be chosen to be of the square root of machine precision for optimal accuracy.

Chapter 3

Code Architecture

The current section aims to explain how the code is structured in the program. We decided to move, as we anticipated in the code specification, to an Object Oriented (OO) paradigm. Designing the OO scheme was not trivial because the problem had to be decomposed into individual objects and the relations between them had to be determined. Nevertheless, in the end it turned out very useful for writing code. More precisely, the code is now much more clear and instead of having all the data storaged in meaningless, large matrices, it is well packed into meaningful objects. Not only does this facilitate writing algorithms in a more natural way, but also makes easier to extend the code in the future provided that the initial structure wisely designed.

As shown in 3.1, the central classes are ParticleSystem and Particle. Most of the Molecular Dynamics code is contained withing ParticleSystem where forces, velocities and positions of the Particle object can be easily accessed. MDSimulation acts as a wrapper for all the configuration options and is in charge of running the main loop, along with doing the appropiate input and output making use of classes inherited from File.

The last important set of classes, are the ones related to the energy of the system. They are contained within ParticleSystem and represent both the bond energy (BondEnergy) and the repulsive energy due to Pauli exclusion (RepulsiveEnergy), which are inherited from Energy abstract class. The main pourpose of Energy-inherited objects is to provide a way of calculating the energy and updating the forces acting on one particle. The kinetic energy of the nucleai comes from their velocity and it is calculated within ParticleSystem. Therefore, it does not inherit from Energy, corroborating the fact that no forces are derived from it. The last important class related to energy is Hamiltonian, which is just a Matrix wrapped with some methods to build it properly.

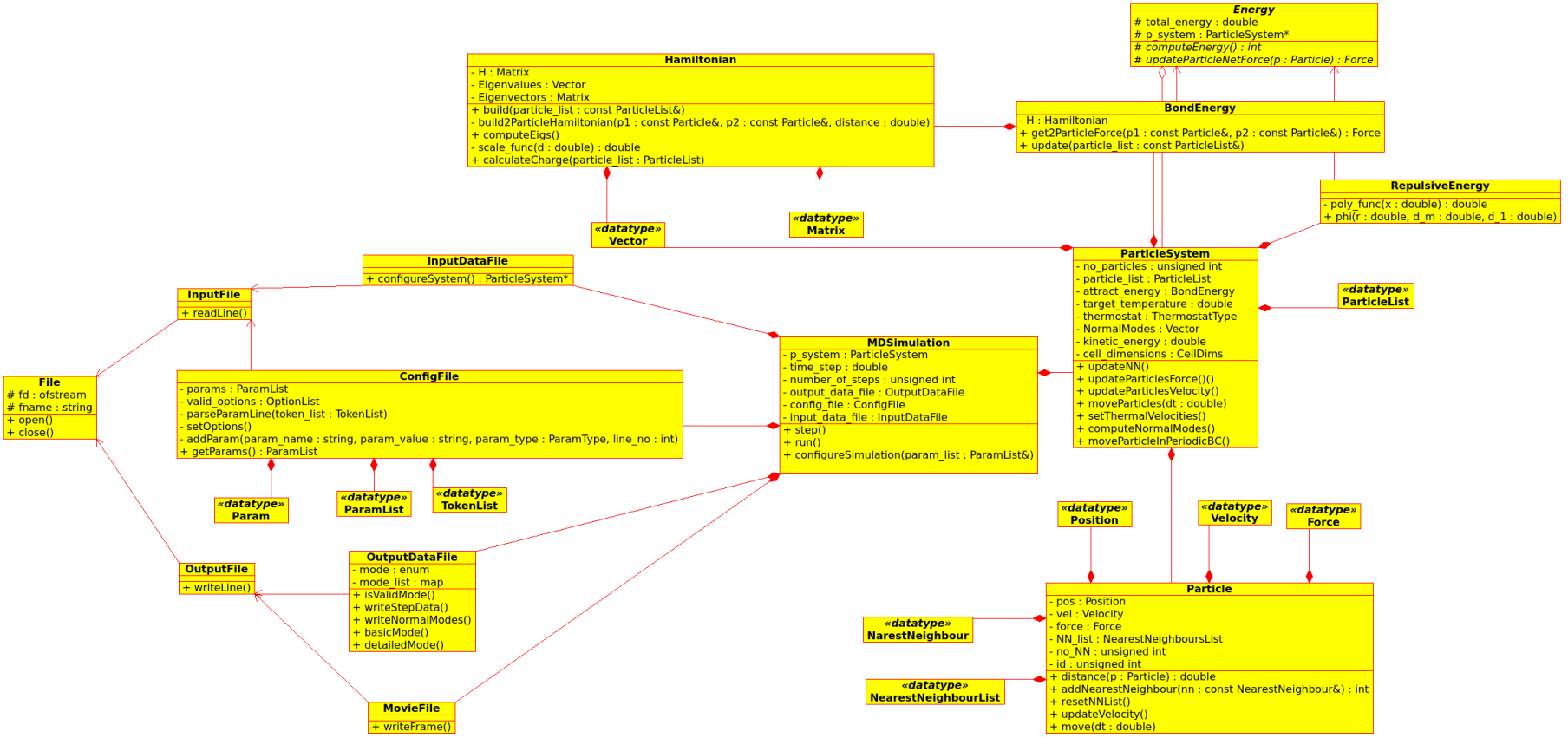

FIGURE 3.1: *UML diagrom of the project.*

Chapter 4

Results and Discussion

4.1 Tests

The code was tested on small molecules of two to ten atoms. Firstly, we made sure that the results of simulations for these molecules did not change under translations and rotations of coordinate system. Secondly, we checked that energy was conserved during the simulation. Additionally we checked the equilibrium configurations of the clusters and compared them to those predicted by Xu et al [11]. These are shown in Fig. 4.3.

As can be seen from Fig. 4.1 for two particles released from rest, energy oscillations were smaller when the initial separation is close to the equilibrium case (1.413 $\mathring{A}$). This is because smaller kinetic energy and velocities lead to a smaller error in integrating equations of motion. The magnitude of these oscillations also decreased if a smaller time-step is used.

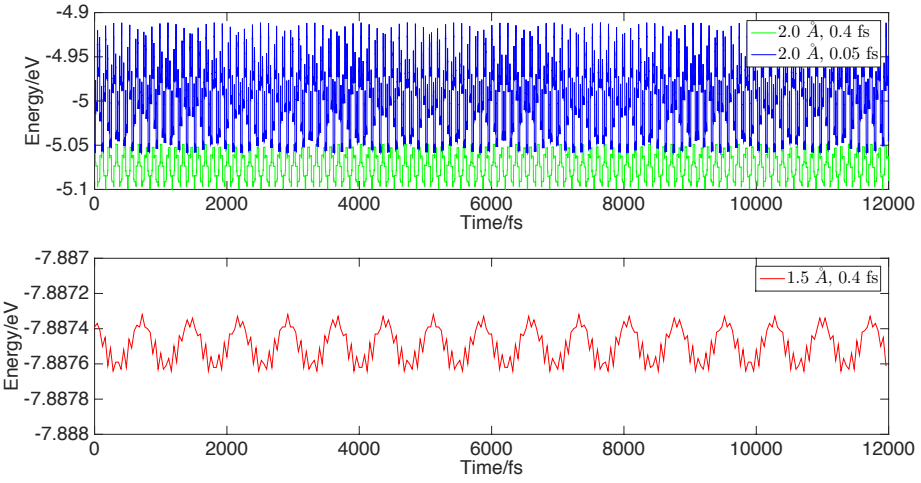

FIGURE 4.1: *The graphs show how energy fluctuates for C2 molecule as a function of time-step and initial separation of atoms (released from rest). Smaller time step and velocities lead to better energy conservation.*

An appropriate step size must be chosen for molecular dynamics simulations. Convergence with respect to the time-step was monitored by initialising the simulation at $T = 1000$ K and equilibrating the input structure of ten atoms, followed by a simulation in constant energy mode (production run). By computing the ratio of the standard deviation per atom to the thermal energy during the production run, it was found (see Fig. 4.2) that a time-step of 0.4 fs was sufficient to ensure that this ratio remained below 0.1 %. This time-step was used in all the following dynamical simulations. The final version of the code containing analytic expressions for derivatives of energy was checked to reproduce the results obtained using numerical derivatives

via central finite difference methods. Detailed information on parameters used for testing and all the relevant results are available in the Appendix A.

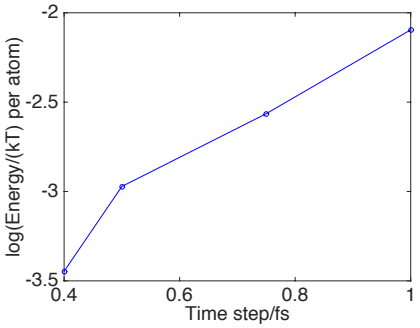

FIGURE 4.2: *The figure shows the standard deviation of the energy as a function of time step for a ring of ten atoms.*

To check the implementation of the tight-binding potential further, we checked the equilibrium bond lengths obtained in our simulations with those in the original paper [11] (quoted in brackets below in the paper). Some clusters have slight disagreements with [11] because the Mulliken charge on each carbon atom is not correct in those clusters. This agrees with the finding in [11], that a Hubbard term should be added to the Hamiltonian in order to account for charge transfer in clusters with less that ten atoms.

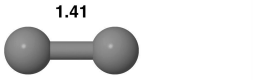

(A) C_2: *Total agreement.*

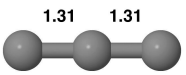

(B) C_3: *Total Agreement.*

(C) C_4: *Disagreement of 0.01 Å.*

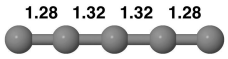

(D) C_5: *Disagreement of 0.02 Å.*

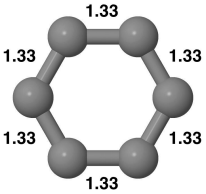

(E) C_6: *Disagreement of 0.03 Å.*

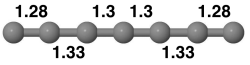

(F) C_7: *Disagreement of 0.03 Å.*

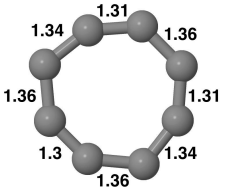

(G) C_8: *Total Disagreement.*

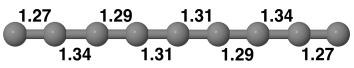

(H) C_9: *Total Agreement.*

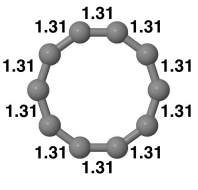

(I) C_{10}: *Total Agreement.*

FIGURE 4.3: *A variety of Carbon chains are shown, along with equilibrium bond-lengths in units of Å for comparison with Ref. [11]. Note that the C_8 structure does not achieve a symmetric equilibrium structure. This can be attributed to the Hubbard term.*

4.1.1 Hamiltonian parametrisation

While testing the on the dynamics of a diatomic carbon molecule, we found an artefact of the parametrisation used for the Hamiltonian. As can be seen from Fig. 4.4 the total force experienced by each atom becomes discontinuous at a distance of around 1.2 $\mathring{A}$. This discontinuity appears in the bonding force because the ordering of eigenvectors according to the energy changes with two eigenvectors being degenerate when the separation is approximately 1.2 $\mathring{A}$.

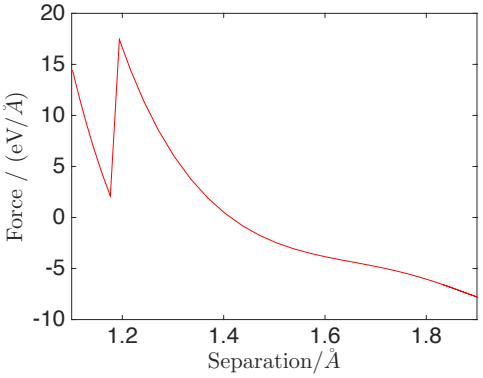

FIGURE 4.4: *The graphs shows force as function of separation for a diatomic carbon molecule. The discontinuity is an artefact of the Hamiltonian parametrisation.*

4.2 Small carbon clusters

The normal modes of small carbon clusters were computed and compared them with results of Kurtz et al [6] in tables 4.1a - 4.1d. From the tables, we see that in many cases relative error is below 10% and several cases of larger deviations can be assigned to the absence of Hubbard term in our Hamiltonian mentioned above, which would give incorrect forces on atoms. Some of these modes are also presented visually in Fig. 4.5.

Mode	Freqeuncy / cm^{-1}		Σ
	TBMD	MBPT [6]	
ν_1 (σ_g)	1216	1220	0.3
ν_2 (σ_u)	1723	2184	21
ν_3 (π_u)	361	190	90

(A) C_3

Mode	Freqeuncy / cm^{-1}		Σ
	TBMD	MBPT [6]	
ν_1 (σ_g)	2092	2150	2.7
ν_2 (σ_g)	932	951	2.0
ν_3 (σ_u)	1456	1588	8.3
ν_4 (π_g)	454	420	8.1
ν_5 (π_u)	186	185	0.3

(B) C_4

Mode	Freqeuncy / cm^{-1}		Σ
	TBMD	MBPT [6]	
ν_1 (σ_g)	645	673	4.1
ν_2 (σ_u)	1231	1244	1.0
ν_3 (σ_g)	1685	1758	4.1
ν_4 (σ_u)	1849	2009	7.9
ν_5 (σ_g)	2173	2166	0.3
ν_6 (π_u)	80	109	27
ν_7 (π_g)	218	224	2.7
ν_8 (π_u)	399	445	10
ν_9 (π_g)	516	548	5.8

(C) C_6

Mode	Freqeuncy / cm^{-1}		Σ
	TBMD	MBPT [6]	
ν_1 (σ_g)	1908	1877	1.7
ν_2 (σ_g)	768	731	5.1
ν_3 (σ_u)	1902	2358	19
ν_4 (σ_u)	1491	1471	1.4
ν_5 (π_g)	329	281	17
ν_6 (π_g)	607	480	27
ν_7 (π_u)	134	131	2.1

(D) C_5

TABLE 4.1: *Normal modes are shown for a range of Carbon structures. MBPT results are obtained from Ref. [6]. $\Sigma = 100 \times$ Relative error.*

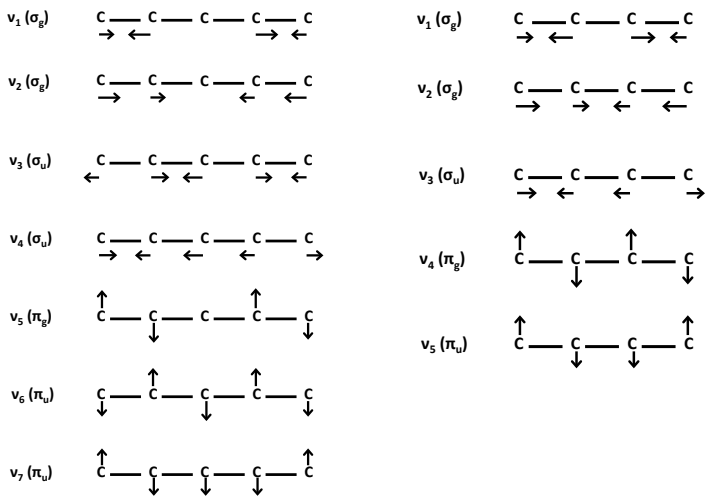

FIGURE 4.5: *Forms of normal modes for C_4 and C_5, which was adapted from [1]*

4.3 Single-Walled Carbon Nanotube

The equilibrium structure of Carbon nanotubes was investigated. For this purpose we wrote a program `nanotube_generator.cc` which produces structures of zig-zag and armchair chirality with diameter and length specified by the user. The program was used to find the equilibrium bond length of a (3,3) single-walled carbon nanotube. The equilibrium bond length was found

by fitting a parabola to the energies produced from the static calculations on the nanotube with 20 repeat units (length 50 $\mathring{A}$, periodic boundary conditions applied). This is shown in Fig. 4.6. The equilibrium bond length was found to be 1.43 $\mathring{A}$ - a value somewhat larger than 1.34 $\mathring{A}$ obtained using self-consistent force field parametrisation by [12]. The Youngs modulus was found by [12] to take values from 1 to 2 TPa depending on the method used - we used the same formula to arrive at the value of 4.4 ± 0.5 TPa.

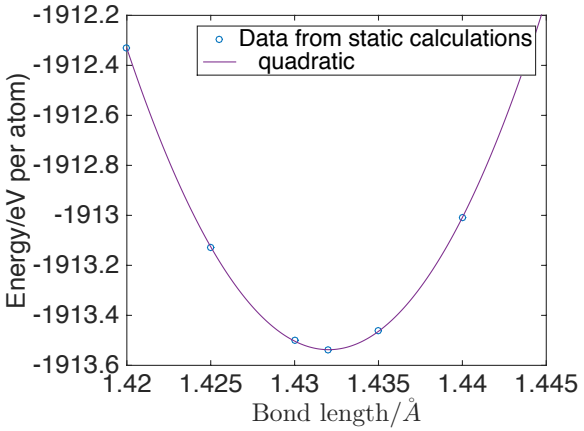

FIGURE 4.6: *The graph shows how the energy of a (3,3) single walled carbon nanotube depends on the bond length between atoms.*

4.4 Buckminsterfullerene

4.4.1 Normal modes

The input structure of a distorted Buckminsterfullerene was relaxed to obtain its equilibrium configuration, which is shown in Fig. 4.7a. At equilibrium the fullerene was found to be symmetric with interatomic distances of 1.46$\mathring{A}$ for the bond length within five-member rings and 1.40$\mathring{A}$ for the bond connecting different five member rings. These compare favourably with results obtained with electron diffraction: 1.458$\mathring{A}$ and 1.401$\mathring{A}$, measured by Hedberg et al [5].

For the equilibrium configuration, 174 normal modes were obtained - as expected for the 180 degrees of freedom (subtracting translational and rotational modes). The 174 normal modes were grouped together by their degeneracy taking values from $[1, 3, 4, 5]$, corresponding to group theoretical labels A, E, T, G and H. We find three A groups, sixteen T groups, twelve G groups and fifteen H groups - as observed experimentally in calculations of Schettino et al [7]. The normal frequencies in each of the A-H groups are compared to those [7] obtained from DFT using the B3-LYP xc-functional in Fig. 4.7. Our results have errors of at most 100 cm^{-1} compared to the DFT results and have reasonable agreement given that the parameters for the repulsive energy and tight-binding potential used were not fitted to reproduce normal modes correctly. The normal modes with degeneracy 1 and 5 agree with more consistently relative to the normal modes with degeneracy 3 and 4.

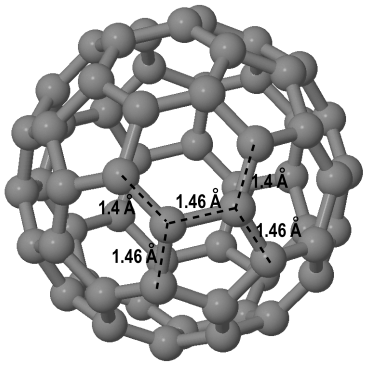

(A) *This is Buckminsterfullerene in its relaxed configuration. The consistency of the bond lengths confirm equilibrium.*

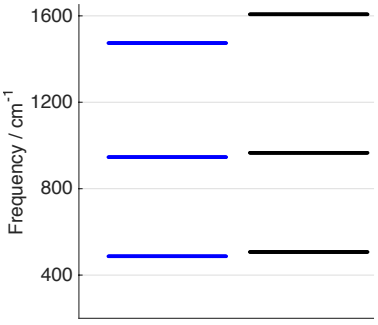

(B) *Degeneracy 1*

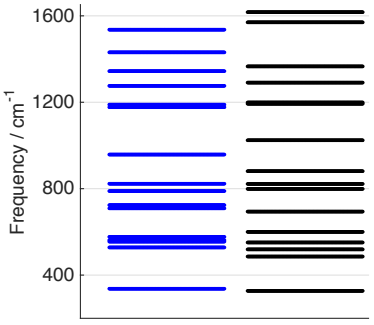

(C) *Degeneracy 3*

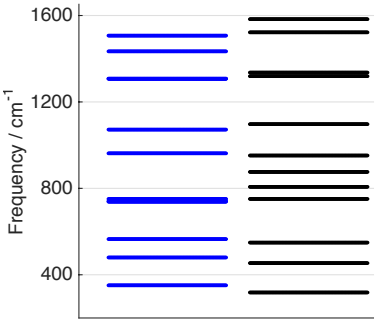

(D) *Degeneracy 4*

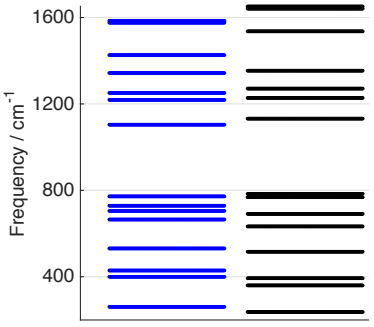

(E) *Degeneracy 5*

FIGURE 4.7: *The vibration spectrum of C60 is shown. The black lines correspond to the prediction made by the TBMD program and the blue lines correspond to DFT results from Schettino et al [7]. There seems to be reasonable agreement between the results especially for normal modes of degeneracy 1 and 5.*

4.4.2 Heat Capacity

Heat capacity of the C60 fullerene was obtained from standard deviation of energy during the MD simulations runs at different temperatures. Five thousand steps were used to equilibrate the initial structure followed by production run of 95000 steps (0.4 fs each) at each temperature

to obtain the statistical data. The results are shown in Fig. 4.8 and can be seen to converge to the value predicted by equipartition theorem at large temperature.

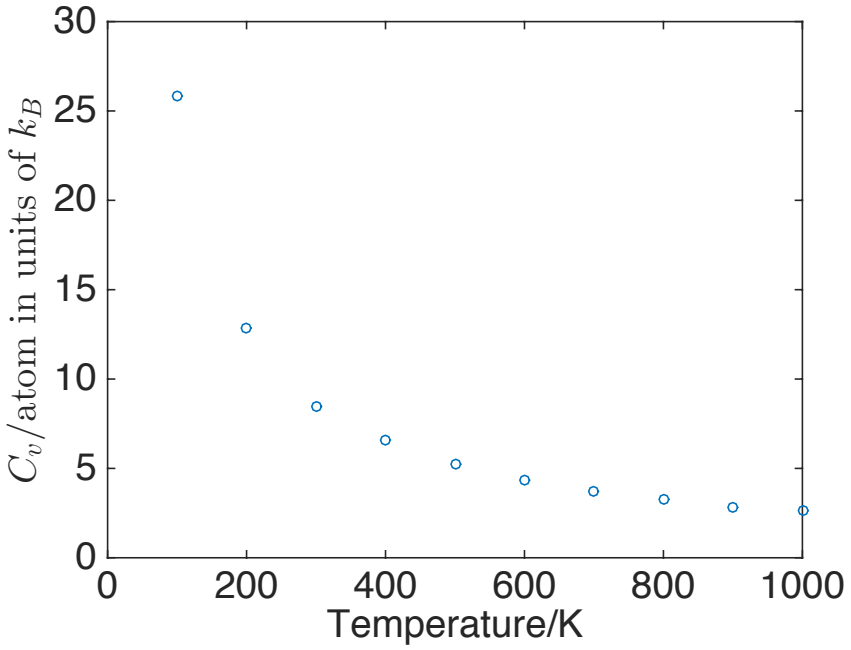

FIGURE 4.8: *Heat capacity of Buckmisterfullerene as a function of temperature. The value at 1000 K equals 2.6 in units of Boltzman constant - close to 3 expected from equipartition theorem.*

4.5 Linear Chain, Diamond and Graphene

For a better comparison among the different structures and with the results reported in Ref. [11], the equilibrium configurations were determined in terms of the nearest neighbour distance (NND) within each compound, namely diamond, graphene and an infinitely long linear carbon chain. At $T = 0$, the equilibrium configurations correspond to potential energy minima. Thus, the total energy of each structure was analysed as a function of the NND to find its respective minimum and hence the equilibrium NND. Since the geometry of each structure had been known in advance, the atomic positions were simply scaled with respect to the NND while applying periodic boundary conditions to avoid any surface effects. We performed calculations using Γ-point sampling and increased the supercell size until the total energy converged to within 0.01 eV/atom. The calculated total energies were then plotted against the respective NND, see Fig. 4.9b, and either a third or fifth order polynomial, depending on the size of the sample sets, was fitted to the data. The equilibrium NNDs, which are presented in Tab 4.2, were straightforwardly found by locating the minima of the relevant fits.

4.5.1 Diamond Heat capacity

The graph 4.10 shows the reduced specific heat of diamond at constant volume. The simulations were performed with 3x3x3 supercell containing 216 atoms. It is apparent that the data scatters a lot and is not very representative. The reason for this is that the runs were not long enough

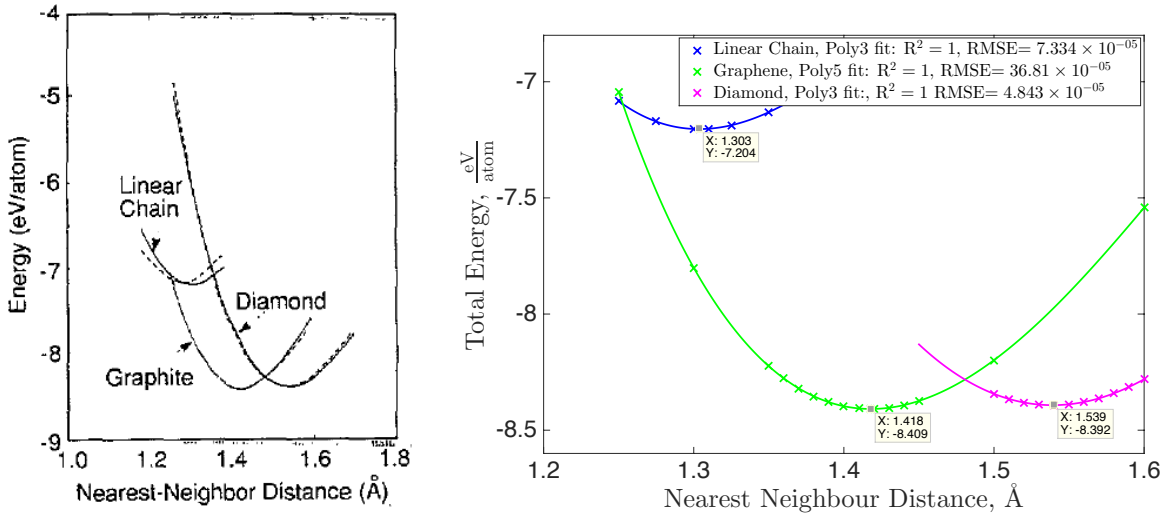

(A) (B)

FIGURE 4.9: *The graph in (A) is the energy vs bond length for different carbon structures which was reproduced from [11]. The energies in (B) were predicted using the program.*

to be fully representative and time pressure did not allow to average over several independent runs. However, the data available shows two interesting features to address here. First, one can see that the high temperature limit heat capacity is of the right order of magnitude, i.e. close to $3k\_B$ per atom. Secondly, the specific heat clearly increases in the low temperature regime with increasing temperature. We stress again, that the absolute values are not representative. In further studies, it would be interesting to study the behaviour of the specific heat at low temperature and to compare it with classical theories like the Debye or Einstein model.

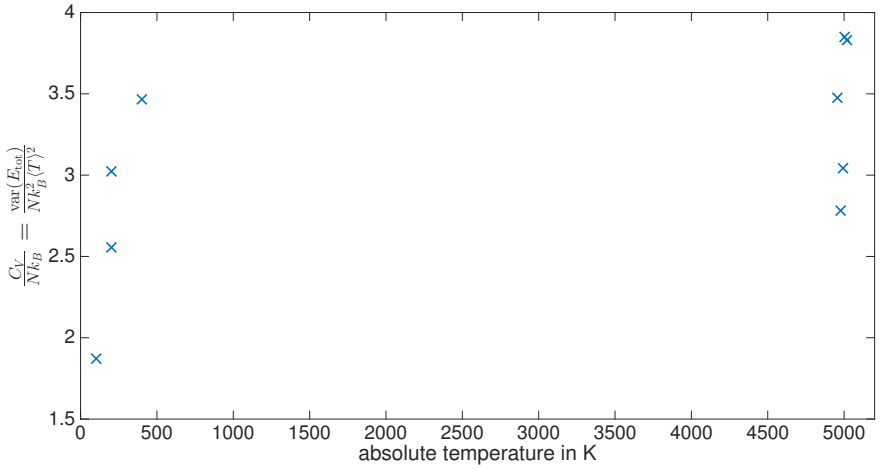

FIGURE 4.10: *Reduced specific heat per atom of diamond as a function of temperature.*

4.5.2 Diamond Elastic Constants

For diamond, we calculated the zero-temperature bulk modulus, B_0 as follows. The definition of the bulk is

$$B_0 \equiv -V\frac{\partial P}{\partial V}\bigg|_{T=0} = V\frac{\partial^2 E_{\text{tot}}}{\partial V^2}\bigg|_{T=0}, \tag{4.1}$$

where V is the unit cell volume and P is the pressure. Thus, with $x = \left(\frac{V}{V_0} - 1\right)$, where V_0 is the equilibrium unit cell volume, it follows that

$$\frac{\partial^2 E_{\text{tot}}}{\partial V^2} = \frac{1}{V_0^2}\frac{\partial^2 E_{\text{tot}}(x)}{\partial x^2} \tag{4.2}$$

and therefore

$$B_0 = V_0\frac{1}{V_0^2}\frac{\partial^2 E_{\text{tot}}(x)}{\partial x^2}\bigg|_{x=0} = \frac{2}{V_0}c_2, \tag{4.3}$$

where c_2 is the coefficient of the second order term of the polynomial fit $E_{\text{tot}}(x) = c_1 x + c_2 x^2 + \cdots + c_n x^n$. For diamond, the associated curve is shown in Figure 4.11. The obtained bulk modulus was $B_0 = 2.9179 \pm 0.0156 \frac{\text{eV}}{\text{Å}^3} \approx 467.5 \pm 2.5$ GPa. This result compares well with the literature value of 443 GPa at T=4 K.

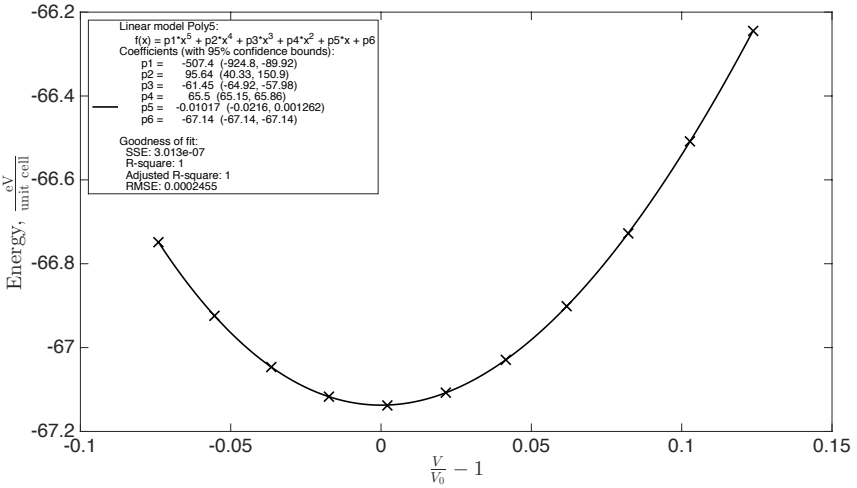

FIGURE 4.11: *The graph shows the total energy of a diamond unit cell as a function of* $x = \left(\frac{V}{V_0} - 1\right)$

The elastic constant difference $C_{11} - C_{12}$ was determined following the method described by Giustino [4], namely

$$C_{11} - C_{12} = \frac{\Delta E_{\text{tot}}}{3\eta^2 V_0}, \tag{4.4}$$

where ΔE_{tot} is the change in total energy of the unit cell due to a compressive strain η along two of the lattice vectors and a tensile strain 2η along the remaining third lattice vector. The obtained result was 616.5 GPa with $\eta = 10^{-3}$ which compares well with 622 GPa, the value reported by Ref. [11].

We were not able to compute C_{44} since our periodic boundary condition only work for the Cartesian coordinate system. Representing the trigonal deformation, i.e. the strain along the body diagonal of the unit cell, in a Cartesian coordinate system is in principle possible but requires an extremely large supercell making the energy calculation impracticable.

Structure	NND_0 / Å	B_0 / GPa	$C_{11} - C_{12}$ / GPa
Diamond	1.53898	467.5 ± 2.5	616.5
Graphene	1.41803	-	-
Linear Chain	1.30353	-	-

TABLE 4.2: *Elastic constants and equilibrium bond lengths.*

Chapter 5

Conclusion

A molecular dynamics program was created to evolve a system of carbon atoms interacting via a semi-empirical tight-binding potential. The program can take many different configurations of carbon atoms and study their time evolution or relaxation. Many different structures were simulated and their properties were investigated.

The program's performance in calculating these properties was reasonable given that the tight-binding potential used was not fitted for all the properties studied.

The normal modes of small carbon clusters were calculated after they had been relaxed to their equilibrium structure. They were compared against normal modes calculated using MBPT and the agreement between the two sets of values was reasonable. Errors were attributed to the fact that our tight-binding potential did not include the Hubbard term as mentioned in Section 4.1. This problem was only present when considering small clusters of carbon atoms.

A single-walled nanotube was investigated and its equilibrium structure was found by plotting the energy of the structure for different bond lengths. The equilibrium structures of diamond, and an infinite linear chain and graphene were also investigated. The resulting equilibrium bond lengths were very close to those calculated via DFT methods in [11].

Additionally the normal modes of the Buckminsterfullerene were calculated showing some agreement with those calculated using DFT. Its heat capacity was investigated for a range of temperatures and was shown to approach the value predicted by the equipartition theorem.

Further investigations into diamond were also made. In particular the bulk modulus was calculated and the heat capacity as a function of temperature was investigated. The bulk modulus was in very good agreement with literature values however due to time constraints we could not sample over enough simulations to correctly calculate ensemble averages for the heat capacity.

Last but not least we would like to summarise what we have learnt from this project which gave us some highs as well as lows. Apart from the scientific concepts which were completely new to at least some of us, the biggest challenge was by far to coordinate the work and tasks in an efficient way. However, the fact that we can say this now is a strong proof that we must have learnt a lot about working on a computational problem as a team rather than as individuals. We were exposed to each others' flavours and preferences of coding and thoroughly enjoyed arguing with and learning from each other. Surely, the knowledge about each others' strengths (and our own weaknesses) will prove useful during our time as PhD students as we will know whom to approach with a particular problem in mind. We are looking forward to working together as a group at some point in time again.

Appendix A

Details of Tests

Convergence wrt time step
Gamma = 0.05 for 1000 fs (found sufficient from observing behavious of energy vs time during equilibration) for equilibration at T=1000 K (OVRVO), followed by production run of 12000 fs.

Initial configuration	Time step/fs	Sigma_E	Sigma_E/(kT*# atoms)	Filename
(2) 1.5 0	0.4	4.836e-05	0.0002806	1
(2) 1.5 0	1.0	0.0001494	0.0008668	2
(2) 1.5 0	2.0	0.001441	0.008361	3
(10) same config as below	0.4	0.0003079	0.0003572	6
(10) same config as below	0.5	0.0009197	0.001066	7
(10) same config as below	0.75	0.002348	0.002724	8
(10) same config as below	1.0	0.006913	0.008019	5
(10) same config as below	2.0	0.01924	0.02232	9

Final tests of the code
In all cases the code tests were performed with the following parameters unless states otherwise:
Gamma = 0.05, dt =0.4, steps 30 000, T=0K (OVRVO), TOL 10^-15
All data was output.dat and movie.xyz files were preserved (as filename .dat or .xyz)

*For the case of two atoms initially separated by 2 A the energy as a function of time was compared with the simulation of other group (using the same parameters) – the resultant curves were identical for the two codes.

(# particles); their coordinates	Energy conservation	TEMPERATURE	ROT & TRANSSYM	Result, bond length/A	File name
(2) (1.2,0,0) (0,0,0)	Oscillations O(10^-3 eV) (Gamma=0)	n/a	Run six simulations putting particles along x, y, z and translating them along these axes	Oscillates	a
(2) (1,0,0) (000)	Not conserved (Gamma=0)	n/a	-	Blows apart (too high initial E)	b
(2) (1,2,3) (1.5,1,2)	Oscillations	n/a	-	Oscillates	c.

(distance 1.5)	O(E-4 eV) (Gamma=0)				
(2) 1.45 and 0 along y	n/a	E-22	All x=-1.0 Z=1.7	1.4134	e
(2) 2 and 0*	Oscillations O(E-2 eV) (Gamma=0)	n/a	All x=-1.0 Z=1.7	Oscillates	f.
(2) 2 and 0		n/a	All x=-1.0 Z=1.7		g
(3) (0,1,0) (1,1,1) (0,0,1)	n/a	E-17	-	Distances 1.310 Charges: 3.95, 4.10, 3.95	d.
(4) -3-1 1.01 3	n/a	E-17	Coord along y All x =0, all z=0.1	As in old test Bonds: 1.75,2.31, 1.25 Charges: 5, 5, 3, 3	4a
(4) -3 -1 0.99 3	n/a	E-17	Coord along y All x =0, all z=0.1	As in old test Bonds: 1.25,2.31, 1.75 Charges 3, 3, 5, 5	4b
(10) p.setPositionByCoords(-2.2, 0.0 ,0.0); p.setPositionByCoords(2.2, 0.0 ,0.0); p.setPositionByCoords(-2.0, 1.3 ,0.0); p.setPositionByCoords(2.0, 1.3,0.0); p.setPositionByCoords(-2.0, -1.3 ,0.0); p.setPositionByCoords(2.0, -1.3 ,0.0); - p.setPositionByCoords(0.8, 2.5 ,0.0); p.setPositionByCoords(-0.7, 2.5 ,0.0); p.setPositionByCoords(0.9, -2.5 ,0.0); p.setPositionByCoords(-	n/a	E-20	-	As in the old test All distances 1.311 All - charges 4.000…	10

0.9, -2.5 ,0.0);					
(4) Z-like with all bonds 1.3	n/a	E-21	-	Linear as in the old All distances 1.32, Charges: 3.8, 4.2, 4.2, 3.8	4c.
(4) Z-like with all bonds 1.3	O(E-3 eV) (Gamma=0)				
(4) perfect square with all bonds = 1.3		E-17	In y-z plane, X=-1.0	Linear as in the olds test All Distances 1.32 Charges: 3.8, 4.2, 4.2, 3.8 (50000 steps)	4d

N.B. some of the movie.xyz files may not be correctly reproduced by jmol

Old tests performed with numerical forces

(4) -3 -1 1.01 3	Same as above	Bonds: 1.75, 2.31, 1.25 Charges: 5, 5, 3, 3
(4) -3 -1 0.99 3	Same as above	Bonds: 1.25, 2.31, 1.75
(4) starting z-like all with all angles = 90 deg and bonds = 1.3	Becomes symmetric	Linear with bonds 1.320, 1.316, 1.320 Charge: 3.8, 4.2, 4.2, 3.8
(4) perfect square with all bonds = 1.3	Becomes symmetric	Linear equilibrium with all bonds 1.32
(4) perfect square with all bonds = 1.1	Splits into 2+2; two different bond lengths	Charges: 5, 5, 3, 3 Bonds: 1.25 and 1.75
(4) perfect square with all bonds = 1.7	Becomes symmetric	Linear with bonds 1.320, 1.316, 1.320 Charges: 4.2, 3.8, 3.8, 4.2
(2) starting with bond = 1.1, 1.5, 1.7, 2.0	(all four final results are the same)	Equilibrium with bond length 1.41 as in the past

(3) -6, -7.5, 6		Charges are 5, 5 and 2, (bond is 1.25 A)
The agreement for 2 and 3 atom molecules is better because charge transfer is smaller there.		

(10):
 	
p.setPositionByCoords(-2.2, 0.0 ,0.0);
particle_system_.addParticle(p);
p.setPositionByCoords(2.2, 0.0 ,0.0);
particle_system_.addParticle(p);
p.setPositionByCoords(-2.0, 1.3 ,0.0);
particle_system_.addParticle(p);
p.setPositionByCoords(2.0, 1.3,0.0);
particle_system_.addParticle(p);
p.setPositionByCoords(-2.0, -1.3 ,0.0);
particle_system_.addParticle(p);
p.setPositionByCoords(2.0, -1.3 ,0.0);
particle_system_.addParticle(p);
p.setPositionByCoords(0.8, 2.5 ,0.0);
particle_system_.addParticle(p);
p.setPositionByCoords(-0.7, 2.5 ,0.0);
particle_system_.addParticle(p);
p.setPositionByCoords(0.9, -2.5 ,0.0);
particle_system_.addParticle(p);
p.setPositionByCoords(-0.9, -2.5 ,0.0);
particle_system_.addParticle(p);
		All bonds equals to 1.3116 A
		(see comment above for 6 particles reg. hexagon)
		charges on all atoms are
		4.000000

Bibliography

[1] DW Arnold, SE Bradforth, TN Kitsopoulos, and DM Neumark. Vibrationally resolved spectra of c2–c11 by anion photoelectron spectroscopy. *The Journal of chemical physics*, 95(12):8753–8764, 1991.

[2] F. Ercolesi. Lecture notes on tight-binding molecular dynamics, and tight-binding justification of classical potential. 1-13, 2005.

[3] S Fahy and Steven G Louie. High-pressure structural and electronic properties of carbon. *Physical Review B*, 36(6):3373, 1987.

[4] F. Giustino. *Materials Modelling Using Density Functional Theory: Properties and Predictions*. Oxford University Press, 2014.

[5] Kenneth Hedberg, Lise Hedberg, Donald S Bethune, CA Brown, HC Dorn, Robert D Johnson, and M De Vries. Bond lengths in free molecules of buckminsterfullerene, c60, from gas-phase electron diffraction. *Science*, 254(5030):410–412, 1991.

[6] Joe Kurtz and Ludwik Adamowicz. Theoretical vibrations of carbon chains C3, C4, C5, C6, C7, C8, and C9. *The Astrophysical Journal*, 370:784–790, April 1991.

[7] Vincenzo Schettino, Marco Pagliai, Lucia Ciabini, and Gianni Cardini. The Vibrational Spectrum of Fullerene C60. *J. Phys. Chem. A*, 105(50):11192–11196, December 2001.

[8] David A. Sivak, John D. Chodera, and Gavin E. Crooks. Time step rescaling recovers continuous-time dynamical properties for discrete-time langevin integration of nonequilibrium systems. *The Journal of Physical Chemistry B*, 118(24):6466–6474, 2014. PMID: 24555448.

[9] A.P. Sutton. *Electronic Structure of Materials*. Oxford Science Publ. Clarendon Press, 1993.

[10] Paul Tangney. langevinmd.m. *TSM-CDT Lecture Course on Methods of Simulating Materials*, 2015. Imperial College London.

[11] C H Xu, C Z Wang, C T Chan, and K M Ho. A transferable tight-binding potential for carbon. *Journal of Physics: Condensed Matter*, 4(28):6047, 1992.

[12] Jin-Liang Zang, Quanzi Yuan, Feng-Chao Wang, and Ya-Pu Zhao. A comparative study of Young's modulus of single-walled carbon nanotube by CPMD, MD and first principle simulations. *Computational Materials Science*, 46(3):621–625, September 2009.